Tidal and Seasonal Variability Circulation Patterns in the Coral Reef System, Berau Continental Shelf, East Kalimantan

Ayi Tarya[1], A. J. F. Hoitink[2] and M. van der Vegt[3]
[1]*Department of Oceanography, Faculty of Earth Sciences and Technology, Bandung Institute of Technology, Bandung 40132, Indonesia*
[2]*Hydrology and Quantitative Water Management Group, Wageningen University, Droevendaalsesteeg 3, 6708 PB Wageningen, The Netherlands*
[3]*Institute for Marine and Atmospheric Research Utrecht/IMAU, Department of Physical Geography, Utrecht University, P.O. Box 80115, 3508 TC Utrecht, The Netherlands*

Keywords: Tidal Variability, Seasonal, Coral Reef System, East Kalimantan.

Abstract: The present study examines tidal and seasonal circulation dynamics in the coral reefs, Berau Continental Shelf, East Kalimantan which exist multiple reef passages by using analysis field data and a three-dimensional hydrodynamic model. The predicted M2 tidal currents, velocities, salinity profiles and sea surface elevation show a good agreement with observed. The model results demonstrate the reef-scale circulation patterns on tidal to monsoonal variation. On the seasonal timescale, the circulation patterns strongly reflect the Monsoon seasonality. The coral reefs exposed by river plume when southwesterly wind prevailed. In this period, the vertical structure of salinity displays a thin stratified water column. The velocity profiles exhibit a classical estuarine circulation with outflow at the top layer and inflow at the bottom layer. For the tidal periods, the tidal currents present complex structures at the reef passages and exhibit the tidal eddies generated by irregularities reef gaps. The flow in the centre of the reef passage is often opposed to the flow near the reef boundaries. A mixed vertically water column occurs during spring tide. During neap tide, the water column structures form a thin stratified on top layer and a classical estuarine circulation for velocity profiles. At the cross-section of reef passages, the lateral velocities develop the two-cell circulation with upward flow at reef shores and an axial convergence (downward flow) at mid-reef passage during flood and reverse pattern during ebb. At the reef slope of continental shelf edge, the model results suggest an upward flow that generated by a Bernoulli effect during flood tide, which may be lifting the nutrient-rich water to the reef passage.

1 INTRODUCTION

Circulation dynamics in coral reef systems can be driven by a number of forcing functions such as waves, tides, wind and density gradients (Andrews and Pickard, 1990; Kraines, 1998; Wolanski, et.al, 1988; Wolanski and Thomson, 1984; Hoitink, 2004; Monismith, et.al, 2006). The associated length scales are ranging from an individual coral colony to the reef, island, and basin scale (Monismith, 2007). In coral reef systems, the hydrodynamics play a crucial role in ecological and biogeochemical processes including dispersal of larval fish and corals (Black, 1993), supply of nutrients to reef organisms (Falter, et.al, 2004), renewal of oxygen (Nakamori, et.al, 1992), delivery of phytoplankton (Yahel, et.al, 1998), the dynamics of zooplankton (Yahel, et.al, 2005), transport of terrigenous sediments (Storlazzi, 2004; Haitink and Hoekstra, 2003), and the distribution of mobile reef fishes (Clarke, et.al, 2005). Therefore, to understand biological and ecological patterns and function in coral reef systems, it is critical to identify the circulation and transport processes.

The importance of wind and waves on circulation patterns in coral reef environments has been investigated extensively (e.g. Wolanski and Thomson, 1984; Hoitink and Hoekstra, 2003; Wolanski and Pickard, 1985; Yamano, et.al, 1998; Presto, et.al, 2006; Kench, et.al, 2009). Wolanski and Thomson (1984), Wolanski and Pickard (1985)) reported that the subtidal sea level dynamics and currents are found to be highly coherent with the local wind variability in the Great Barrier Reef. Trade wind-driven processes are found to be the dominant

Tarya, A., Hoitink, A. and van der Vegt, M.
Tidal and Seasonal Variability Circulation Patterns in the Coral Reef System, Berau Continental Shelf, East Kalimantan.
DOI: 10.5220/0008372500090015
In *Proceedings of the 6th International Seminar on Ocean and Coastal Engineering, Environmental and Natural Disaster Management (ISOCEEN 2018)*, pages 9-15
ISBN: 978-989-758-455-8

control for circulation and sediment dispersal on the shallow, broad reef flats off southern Molokai, Hawaii (Presto, et.al, 2006). The interaction between tides, local bathymetry, coral reef shape, size and spacing can result in periodic reef-scale flow patterns, featuring tidal jets, eddies and circulation cells across the reef passage (Wolanski, et.al, 1988; Wolanski and Hamner, 1988; Young, et.al, 1994; King and Wolanski, 1996). Using a regional model with a 2 km resolution, (King and Wolanski, 1996) established that such local features result from flow interaction with complex topography. Local residual flows may impact the fate of river effluents reaching coral reef areas, which pose a contemporary threat to the health of coral reefs. The reef chain under study features a monsoonal pattern exposed to river plume spreading (Tarya, et.al, 2015). (Tarya, et.al, 2018) revealed that the coastal ecosystem communities at the BCS are most exposed to low salinity when southwesterly winds are prevalent, at neap tide. These findings motivate the present study to further investigate the circulation patterns on the coral reef-scale and on the intratidal periods. In this contribution, we focus on the detailed circulation processes across the reef passages at the BCS, over a tidal cycle.

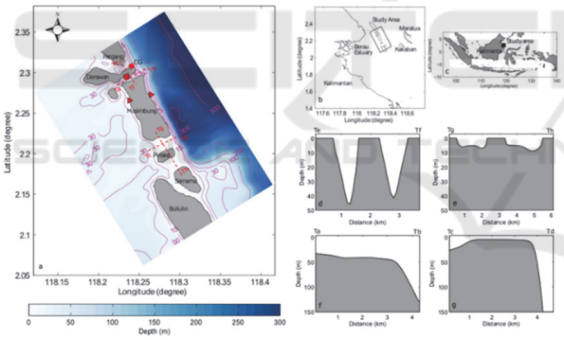

Figure 1: Map of the Berau barrier reef (a), showing depth in meters. Berau Continental Shelf and the position of the Berau barrier reef (b) and map of Indonesia (c). The dashed red line Te-Tf and Tg-Th indicates the location of the depth profile across-northern passages (d) and across-southern passages (e), respectively. The dashed red line Ta-Tb and Tc-Td are depth profile along the northern (f) and southern passage (g), respectively. The red circles indicate fixed ADCP and CTD stations near Derawan Island. Red triangles indicate fixed ADCP stations at Masimbung inner shelf and Masimbung outer shelf. The red square indicates the sea surface elevation at CG station.

2 STUDY AREA

The Berau barrier reef is a juxtaposition of permanent and periodically exposed reef islets at the edge of the BCS, East Kalimantan (Figure 1). It features a species-rich coral reef ecosystem (Hoeksema and Suharsono, 2004; Renema, 2006; Renema, 2006; Voogd and Becking, 2009), which is part of the Coral Triangle in the central Indo-West Pacific (Tomascik, et.al, 1997; Hoeksema, 2007). The islets are elongated in the along-shelf direction, and are separated by 0.8 to 3 km wide passages with depths between 5 and 50 m (Figure 1d and 1e). In the northern areas of the barrier reef, passages can be as deep as 50 m, whereas in the south the depths in the passages are less than 15 m. The reef flats emerge only during low water spring tide. The inner shelf separating the barrier reef from the Berau estuary is about 30 km wide. Depths in that area are typically around 30 m. Figures 1f and 1g show typical bottom profiles across the passages. The northern passage has a depth of about 50 m and in the southern passage, the depth is in the order of 10 m or less. Further seaward, the shelf break is located with a very steep bottom slope. Corals are found across a water gradient from fluvially influenced to fully oceanic conditions. Inshore, reefs feature a relatively low coral cover, with high densities of filter feeders such as sponges, soft corals and crinoids (Renema, 2006). Coral rubble in the areas close to the mainland is often covered by fine mud and silt, with a terrigeneous origin. The outer shelf reef is comprised of diverse reef types, dominated by dense stands of corals and coarse sand (Renema, 2006).

3 METHODS

3.1 Field Surveys

Flow velocities, sea surface elevations and meteorological data were gathered during three field campaigns in the period between September 2006 and February 2008. Acoustic Doppler current profiler (ADCP) surveys were collected with an RD Instruments Broadband 1200-kHz ADCP, pinging at 2 Hz over 60 depth cells with a size of 0.5 m. The ADCP transducer was mounted approximately 0.5 m below the sea surface, and had a 0.5 m blanking distance. The survey boat sailed at a speed of approximately 2 m/s. As a result of the extremely clear water conditions, ADCP backscatter rapidly decreased with depth, limiting the observation range to 15 m. Repeated transect measurements were carried out across several cross-sections in a northern and a southern reef passage. The track length was chosen to include the largest number of cross-sections that could be covered within about 1.5 hours, such

that each location on the track was repeated 10 times within an M2 tidal cycle.

3.2 Hydrodynamic Model

The simulations were performed using the Princeton Ocean Model (POM) (Blumberg and Mellor, 1987). This is a three-dimensional, terrain-following finite difference model based on sigma-coordinates, which solves for water level, velocity, temperature, salinity, turbulence kinetic energy and macro-scale turbulence properties. The model adopts the turbulence closure scheme by (Mellor and Yamada, 1982) to parameterise vertical mixing and uses the (Smagorinsky, 1963) diffusivity formulation for horizontal diffusion. POM has been used in a variety of oceanic and coastal applications including coral reef systems (e.g. Ezer, et.al, 2005; Ezer, et.al, 2010).

The local model was nested in the existing regional model by (Tarya, et.al, 2015) and features a 200 × 200 horizontal orthogonal curvilinear grid, with a resolution ranging from 40 m at reef passages to about 100 m at the outer shelf. 15 sigma levels were defined at 2, 4, 6, 8, 10, 15, 25, 40, 50, 60, 70, 80, 90, 95 and 100% of the water depth. The depth of each grid cell in the reef environment was interpolated from bathymetry data measured during a field survey. Depths in the parts of the domain that cover the shelf and deep sea areas were derived from the Indonesian Naval Hydro-Oceanographic Office (DISHIDROS). A computational time step of 1 s was used for the external mode, while the internal mode time step was set to 10 s.

Sea surface elevation, currents, temperature and salinity at the open boundaries were obtained from the BCS regional model (Tarya, et.al, 2015). The sea surface elevation and momentum variables were implemented adopting the radiation condition of (Orlanski, 1976) that allows incoming waves to freely propagate into the domain, and pass out to the exterior without any reflection back into the computational domain. Time-variable winds are imposed uniformly over the domain model. Hourly observations were collected from Derawan station (see Figure 1) for the period from March 2007 to January 2008, while the wind data for the period February 2006 to January 2007 was extracted from the NCEP reanalysis database, provided by the National Oceanic and Atmospheric Administration (NOAA) (www.esrl.noaa.gov/psd).

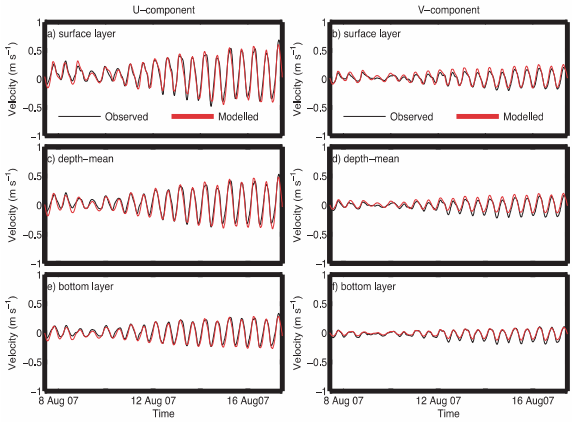

Figure 2: Modelled and observed comparison for surface layer (a and b), depth-mean (c and d) and bottom layer (e and f) velocity for east (left panels) and north direction (right panels) components of the flow near Derawan (see Figure 1).

4 RESULTS

4.1 Comparison of Model Results and Measurements

Modelled sea surface elevation, velocity profiles and salinity were compared with observations to evaluate the performance of the model. Figure 2 present time-series of observed and modelled velocity for the surface layer, the depth-averaged and the bottom layer near Derawan Island. Model performance is quantified by the Mean Absolute Error (MAE), the Root Mean Square Error (RMSE) and the Correlation Coefficient (CC) (Liu, et.al, 2009; Vested, et.al, 2013) as displayed in Table 1. The CC score between modelled and observed values of sea surface elevation is 0.95. RMSE and MAE are 0.08 m and 0.09 m, respectively. The modelled velocity profiles reveal a CC score above 0.86; MAE and RMSE are lower than 0.14 m/s. For the salinity profiles, the CC score is above 0.86. MAE and RMSE are less than 0.1 psu. Overall, model-data comparisons have shown that the model performs well in reproducing the observations.

Table 1: Validation model results with observations based on the Mean Absoulte Error (MAE), Root Mean Square Error (RMSE) and Correlation Coefficient (CC).

Location	Parameter	Layer	Period	MAE	RMSE	CC
Derawan	Salinity	Surface	8 Aug 07	0.04 psu	0.08 psu	0.87
		Middle	8 Aug 07	0.04 psu	0.07 psu	0.91
		Bottom	8 Aug 07	0.03 psu	0.05 psu	0.95
	Salinity	Surface	14 Aug 07	0.05 psu	0.06 m/s	0.94
		Middle	14 Aug 07	0.03 psu	0.05 m/s	0.93
		Bottom	14 Aug 07	0.03 psu	0.04 m/s	0.95
Derawan	East velocity	Surface	7-17 Aug 07	0.07 m/s	0.09 m/s	0.93
		Middle	7-17 Aug 07	0.10 m/s	0.13 m/s	0.84
		Bottom	7-17 Aug 07	0.05 m/s	0.04 m/s	0.96
	North velocity	Surface	7-17 Aug 07	0.04 m/s	0.05 m/s	0.92
		Middle	7-17 Aug 07	0.05 m/s	0.06 m/s	0.81
		Bottom	7-17 Aug 07	0.03 m/s	0.03 m/s	0.94

4.2 Seasonal Circulation Dynamics

The Figure 3 describes the mean circulation and salinity patterns for the surface layer demonstrate a monsoonal pattern. During the transition from the Northwest to the Southeast Monsoon (Figure 3a), the south westerly wind generates the residual northeast flow toward the coral reefs. The vertical structure of velocity exhibits a classical estuarine circulation with offshore flow in a low- density top layer and inshore flow in the bottom layer, for both reef passages (Figure 4).

During the Southeast Monsoon (Figure 3b), the steady southerly winds drive northward residual currents aligned with the barrier reef. In this period, there are no freshwater influences in the barrier reef area. The wind changes from southerly to northerly

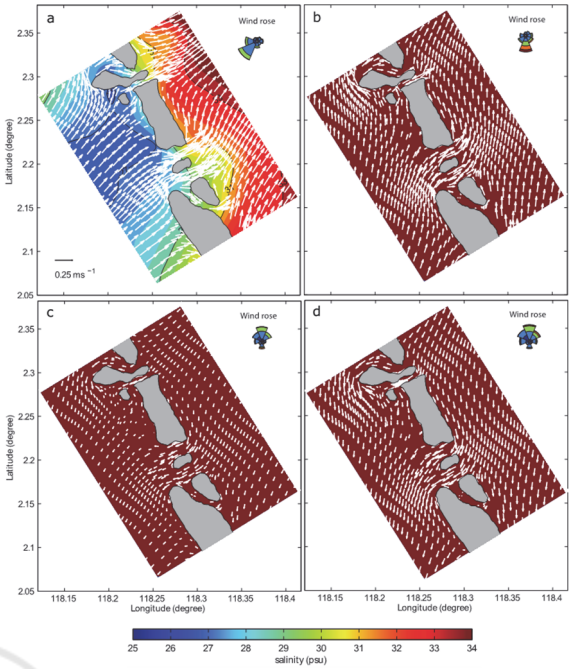

Figure 3: Seasonal pattern of salinity and velocity in the surface layer during transition from the Northwest to the Southeast Monsoon (a), the Southeast Monsoon (b), the transition from the Southeast to the Northwest Monsoon (c), and the Northwest Monsoon (d).

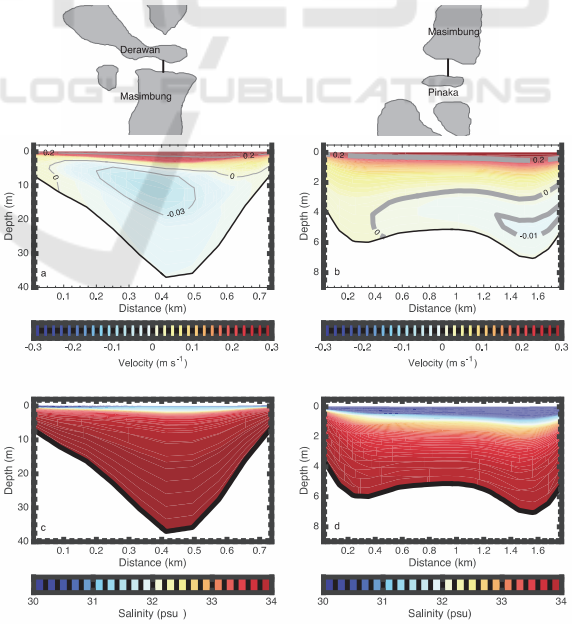

Figure 4: Modelled mean velocity profiles during the transition from the Northwest to the Southeast Monsoon in cross-sections of the northern reef passage between Derawan and Masimbung (a) and the southern reef passage between Masimbung and Pinaka (b). The bottom panels show the corresponding salinity field. The locations of the transects are indicated in the top plots.

during the Southeast to Northwest Monsoon transition. This shifts the surface circulation patterns from northward to southward flow (Figure 3c). Subsequently, the currents through the reef passages weaken and reverse from offshore to inshore. Although the wind is relatively weak during this period, it is effective in dispersing the river plume to the south of the BCS (Tarya, et.al, 2010) and thus the reef passages present vertically uniform seawater and homogeneous velocity profiles directed inshore. During the Northwest Monsoon (Figure 3d), the mean circulation and mean salinity patterns are similar to those in the transition period, but the flow is stronger due to increased northerly wind speed.

4.3 Seasonal Circulation Dynamics

4.3.1 Horizontal Structures

Figure 5 displays depth-mean instantaneous velocity patterns over a tidal cycle in two reef passages. The asymmetric topography of the barrier reef causes flood flow patterns to deviate from the ebb flow patterns. This holds especially in the northern passage (Figure 5 left panels), where several eddies are created in the lee of reef outcrops. The flow in the center of the reef passage is often opposed to the flow near the reef boundaries. The reef waters are subject to tidally-driven flow separation and transient eddy development, as observed previously by (Pingree, 1978; Black and Gay, 1987; Signell and Geyer, 1991). Reef outcrops can act as headlands, generating an adverse pressure gradient where the laterally confined flow diverges and decelerates again.

4.3.2 Vertical Structures

Figures 6 illustrates streamwise and lateral velocities for peak flood and peak ebb during spring and neap tides, across the northern reef passage. The flow structure presents a distinctive temporal evolution over a tidal cycle. During spring tide, along-channel velocities attain magnitudes above 1 m/s, which causes strong vertical mixing, preventing stratification. The lateral flow structure exhibits a two-cells pattern with surface flow convergence toward the middle of the passage and bottom flow divergence. The secondary circulation reverses during ebb. For neap tide, along-channel velocities become weaker and allow stratification. The same two counter-rotating cells of lateral circulation on either side of the channel axis are evident at neap tide. However, the flow magnitude is reduced compared to spring tide conditions.

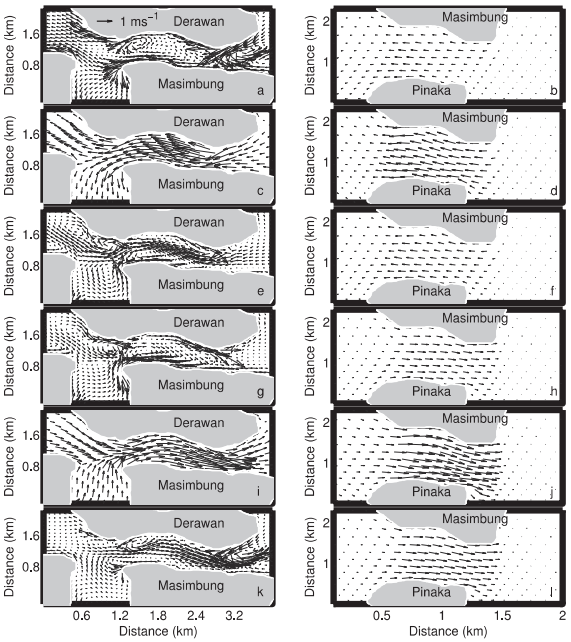

Figure 5: Depth-mean velocity structure during spring tide at early flood (a,b), maximum flood (c,d), late flood (e,f), early ebb (g,h), maximum ebb (i,j), and late ebb (k,l) in northern (left panels) and southern reef passages (right panels).

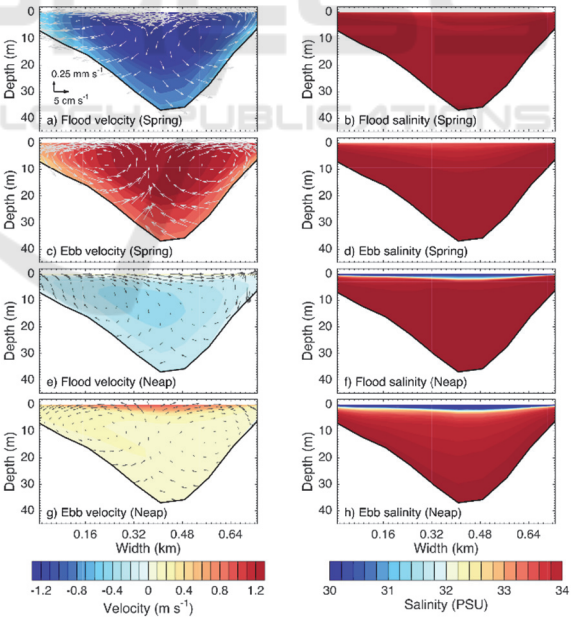

Figure 6: Flow velocities (a,c,e and g) and salinity (b,d,f and h) for a cross-section in northern passage during spring tide and neap tide. The transect is the same as in Figure 5. Colors in the left panels indicate along-reef velocity in the passage. Red indicates offshore flow and blue represents flow toward the inner shelf. Arrows display lateral and vertical velocity components. Color in right panels indicates salinity.

5 DISCUSSION

The south westerly wind during the transition period drives a north eastward flow that pushes the river plume to the barrier reef and results in reef exposure to terrestrial contaminants. The Northwest Monsoon induces a southward residual current that conveys seawater from the open sea. This sequence is essential for flushing of poor quality water. The importance of wind-driven flow to the survival of corals was previously demonstrated by (Kitheka, 1997), who found that the onshore wind-driven flow traps the brackish plume along the south- western coast of the Gazi Bay in Kenya. This ensures that turbid water from the rivers does not reach the coral reef ecosystem in Gazi Bay. Wind induced circulation patterns that play a role in flushing of poor quality water was also reported for the Florida Keys coral reefs (Smith, 2009).

The present study highlights two important processes in coral reef circulation. First, coral reefs that possess a highly irregular shoreline and bottom generate eddies (Pingree and Maddock, 1978). Over time these eddies grow and decay with tidal phases and result in a non-uniform residual flow field. This asymmetry in flow creates a potentially longer retention time of water masses in certain areas around the reef. The generation of the eddies has been proposed as an important physical mechanism that may limit the dispersion of larvae due to the recirculating properties of the water masses that trap and conserve propagules near reefs.

Second, lateral velocity shear in a reef passage with longitudinal density gradients produces the two-cell secondary circulation patterns that form a mid-channel axial convergence and divergence zone over a tidal cycle (Nunes, 1985). The present results highlight the secondary flow structure in the reef gaps during ebb tide and suggest that the water masses of the river plume may be advected in a downward direction leading to additional exposure of the reefs. This process occurs at the shallow reef gaps during neap tides when stronger buoyancy forcing exists.

6 CONCLUSIONS

Coral reefs that possess a highly irregular shoreline and bottom generate eddies. Over time these eddies grow and decay with tidal phases and result in a non-uniform residual flow field limiting the dispersal of larvae. Lateral velocity shear in a reef passage with longitudinal density gradients produces the two-cell secondary circulation patterns that form a mid-channel axial convergence and divergence zone over a tidal cycle.

ACKNOWLEDGEMENTS

This work was partially funded by Research, Community Service and Innovation, Bandung Institute of Technology (P3MI-ITB 2018). The fieldwork was part of the East Kalimantan Programme (EKP) funded by WOTRO Science for Global Development, a division of the Netherlands Organisation of Scientific Research (NWO) under grants WT77–204.

REFERENCES

A. Blumberg, G. L. Mellor, 1987. Three-Dimensional Coastal Ocean Models, Amer. Geophys. Union, Washington D.C, *Coastal and Estuarine Sciences 4, pp. 1–20.*

A. Tarya, A. J. F. Hoitink, M. Van der Vegt, 2010. *J. Geophys. Res. 115*, c09029.

A. Tarya, A. J. F. Hoitink, M. Van der Vegt, M. van Katjwijk, B. Hoeksema, T. Bouma, L.P.M. Lamers, M.J.A. Christianen, 2018. *Cont. Shelf Res. 153, 1*.

A. Tarya, M. Van der Vegt, A.J.F. Hoitink, 2015. *J. Geophys. Res. 120, 16*.

A. J. F. Hoitink, 2004. *Marine Geology 208, 13*.

A. J. F. Hoitink, P. Hoekstra, 2003. *Estuarine Coastal Shelf Sci. 58, 743*.

B. Hoeksema, Suharsono, D. Cleary, 2004. Marine biodiversity of the coastal area of the Berau region, East Kalimantan, Indonesia. Progress report East Kalimantan Program– Pilot phase (October 2003), Naturalis, *Leiden, 2004*, pp. 7–16.

B. King, E. Wolanski, 1996. *J. Mar. Syst. 9, 187*.

B. W. Hoeksema, in Biogeography, Time, and Place: Distributions, Barriers, and Islands, 2007. edited by W. Renema, *Springer Netherlands, Dordrecht, pp. 117–178*.

C. D. Storlazzi, A.S. Ogston, M. H. Bothner, M. E. Field, M. K. Presto, 2004. *Cont. Shelf Res. 24, 1397*.

E. Wolanski, E. E. Drew, A. K. M., J. O'Brien, 1988. *Estuarine Coastal Shelf Sci. 26, 169*.

E. Wolanski, G. L. Pickard, 1985. *Coral Reefs 4, 47*.

E. Wolanski, R. E. Thomson, 1984. *Estuarine Coastal Shelf Sci. 18, 271*.

E. Wolanski, W. M. Hamner, 1988. *Science 241, 177*.

G. Yahel, A. Post, K. Fabricius, D. Marie, D. Vaulot, A. Genin, Limnol. 1998. *Oceanogr. 4, 551*.

G. L. Mellor, T. Yamada, 1982. *Rev. Geophys. Space Phys. 20, 851*.

H. Yamano, H. Kayanne, N. Yonekura, H. Nakamura, K. Kudo, 1998. *Coral Reefs 17, 89*.

H. J. Vested, J. W. Nielsen, H. R. Jensen, K. H. Kristensen, 2013. Quantitative Skill Assessment for Coastal Ocean Models, *American Geophysical Union, pp. 373–396.*
I. Orlanski, 1976. *Journal of Computational Physics 21, 251*.
I. Young, K. Black, M. Heron, 1994. *Cont. Shelf Res. 14, 117*.
J. Falter, M. Atkinson, M. Merrifield, *Limnol. 2004. Oceanog. 49, 18*.
J. Smagorinsky, 1963. Mon. *Weather Rev. 91, 99*.
J. C. Andrews, G. L. Pickard, 1990. Coral Reefs, edited by Z. Dubinsky. *Elsevier, Ecosystems of the world 25, chap. 2, pp. 11–48*.
J. U. Kitheka, 1997. *Estuarine Coastal Shelf Sci. 45, 177*.
K. P. Black, 1993. *Coral Reefs 4, 201*.
K. P. Black, S.L. Gay, 1987. *J. Geophys. Res. 92*, 9514.
M. Presto, A. Ogston, C. Storlazzi, M. Field, 2006. *Estuarine Coastal Shelf Sci. 67, 67*.
N. de Voogd, L. Becking, D. Cleary, 2009. *Mar. Ecol. Prog. Ser. 396, 169*.
N. P. Smith, 2009. *Cont. Shelf Res. 29*, 362.
P. Kench, K. Parnell, R. Brander, 2009. Mar. *Geol. 266*, 91.
R. Nunes, 1985. J. Simpson, *Estuarine Coastal Shelf Sci. 20,* 637.
R. Signell, W.R. Geyer, 1991. *J. Geophys. Res. 96*, 2561.
R. Yahel, G. Yahel, A. Genin, 2005. *Coral Reefs 24, 75*.
R. D. Clarke, E.J. Buskey, K.C. Marsden, 2005. Mar. *Biol. 146*, 1145.
R. D. Pingree, L. Maddock, 1978. Deep Sea Res. 25, 53.
S. Monismith, A. Genin, M. Reidenbach, G. Yahel, 2006. J. Koseff, *J. Phys. Ocean. 36, 13*.
S. B. Kraines, 1998. *Coral Reefs 17, 133*.
S. G. Monismith, 2007. *Annual Review of Fluid Mechanics 39, 37*.
T. Ezer, D. V. Thattai, B. Kjerfve, W. D. Heyman, 2005. *Ocean Dynamics 55, 458*.
T. Ezer, W. D. Heyman, C. Houser, B. Kjerfve, 2010. *Ocean Dynamics 61, 581*.
T. Nakamori, A. Suzuki, Y. Iryu, 1992. *Cont. Shelf Res. 12, 951*.
T. Tomascik, A. J. Mah, A. Nontji, M. K. Moosa, 1997. The Ecology of the Indonesian Seas, Vol. 7 of The Ecology of Indonesia Series, *Periplus Editions (HK) Ltd., Singapore, 1388 p.*
W. Renema, 2006. *Coral Reefs 25, 351*.
W. Renema, 2006. Mar. *Micropaleontol. 58, 73*.
Y. Liu, P. MacCready, B. M. Hickey, E. P. Dever, P. M. Kosro, N. S. Banas, 2009. *J. Geophys. Res. 114*, c00B04.